On the break-up times and lengths of diesel sprays

A. J. Yule
Department of Mechanical Engineering, UMIST, Manchester, UK

I. Filipovic
Department of Mechanical Engineering, University of Sarajevo, Yugoslavia

Measurements of the break-up zone characteristics are reported for simple orifice, direct-injection diesel injectors operating with commercial pumps and injecting into high pressure gas. The difficulty of using photography in this high density region leads to the use of indirect techniques for estimating break-up length. These include the computation of the overall void fraction of the spray, as a function of time, and curve fitting a new penetration rate correlation that incorporates break-up time as an adjustable empirical constant. A combination of theory and dimensional analysis is used to derive three interrelated equations for break-up time, break-up length, and characteristic velocity in the break-up zone. This latter velocity is less than the theoretical injection velocity due to the drag forces on the "intact liquid column" near to the injector orifice. The new equations are in excellent agreement with the present data, and they are also in good agreement with published data obtained from "break points" in penetration rate curves using an idealized constant fuel pressure, impulsively started injection apparatus. Published conductivity probe measurements of break-up length are consistently 35 percent of lengths predicted using the equations. This is expected as the conductivity probe technique measures the intact liquid length, which is shorter than the total break-up length.

Keywords: diesel injection; atomization; fuel sprays; liquid column breakup

Introduction

It is now commonly accepted that the column of fuel, emerging from a simple orifice diesel injector, may require a distance to atomize fully (the "break-up length") that has the same order of magnitude as the distance from the nozzle to the position at which impingement may occur on the piston wall. This concept of a gradual atomization process, at high injection velocities (of the order of 200 m/s) and small orifices (0.2–0.5 mm diameter), was recognized in the early work of Castleman[1] who proposed that atomization, under these conditions, proceeds by the stripping of small ligaments from the liquid column. This fundamentally opposed the received concept of "instantaneous atomization" at the orifice proposed by Haenlein[2] and others. However, this instantaneous atomization concept has persisted until comparatively recently, and it is only after the investigations of Hiroyasu's group[3,4] and work contemporary with that described by Yule *et al.*,[5,6] Ishikawa and Murakami,[7] and others that the importance of the break-up zone has been accepted. When applying computational fluid dynamics (CFD) models to in-cylinder flows it is known that a submodel of the break-up zone is desirable if not essential. This is confirmed by both the work of O'Rourke and Bracco[8] and also the CFD research at UMIST under Watkins.[9,10] Reitz[11] has discussed methods of modeling the break-up zone, but a reliable scheme has still to be developed.

Both qualitative and quantitative information on the break-up zone, as a function of initial and boundary conditions, is scarce. One would hope that photographic and holographic studies could provide such information. Unfortunately, because the outer part of the initial liquid column appears to commence disintegration immediately after it emerges from the orifice, optical penetration of the inner, poorly atomized core of the break-up zone appears to be impossible without severe multiple scattering. This produces ambiguity when attempting to interpret light scattering measurements. This problem was also addressed in the laser velocimetry investigations of Yule and Aval[12] and Pitcher and Wigley.[13] In each of these cases the results were consistent with the existence of a poorly atomized central core, surrounded by a dense peripheral zone of droplets and ligaments. At an injection velocity lower than that used in practical systems (50 m/s or less), and for injection into air at atmospheric conditions, the break-up process is very gradual (extending to several hundred nozzle diameters) and relatively few droplets smaller than 50 μm may be produced. Under these conditions break-up is quite clearly visible and generally involves the, apparently chaotic, occurrence of sheets and longitudinal ligaments. Ishikawa and Murakami[7] used a crossflow of gas under these conditions to reveal the central break-up zone more clearly. However, these observations may be misleading if extended to practical injection conditions where very much larger aerodynamic forces occur and where, for example, the most amplified instability wavelengths, for the surface of the initial liquid column, are very short (of the order of 100 μm).

Aval[14] used a high velocity gas cross flow (up to 50 m/s) with injection into gas at engine conditions. Clear photographs of the break-up zone were not possible, but the low deflection of the upwind side of the spray, near the nozzle, confirmed the existence of this zone. Laser sheet lighting of diesel sprays has been investigated by Ragucci *et al.*,[15] and Zanelli[16] has deduced

Address reprint requests to Dr. A. J. Yule at the Thermodynamics and Fluid Mechanics Division Mechanical Engineering Department, UMIST, P.O. Box 88, Manchester M60 1QD, UK.

Received 26 March 1991; accepted 11 November 1991

the existence of the break-up zone from computer-enhanced photographs. However, in each case the ambiguity of interpretation of optical observations of this zone was recognized. The main body of quantitative data on the break-up zone has been derived from "break points" deduced from penetration rate curves and from conductivity probe measurements using water sprays. Arai *et al.*[4] and Xu and Hiroyasu[17] have presented these results, as is described in the section on the break-up zone structure. In general, their results have been obtained using special injection systems that maintain a constant fuel supply pressure after needle opening. The present paper further extends the database, using several techniques, to practical pump-injector combinations. Relationships for the important parameters of the break-up zone are deduced and comparisons are made with the earlier published data.

Experiments

Diesel injection experiments at UMIST have used single-hole diesel injectors operated with commercial pumps. Table 1 summarizes the operating conditions for three nozzles and the boundary conditions that were used to provide the penetration rate measurements that are reported here. Measurements were made in pressurized gas chambers with, in the case of the nozzle with $D_N = 0.265$ mm, a variable cross-flow velocity W_g, as shown in Figure 1. All measurements used here were made at a gas temperature 290 K $\pm$ 5 K. Measurements at elevated temperatures by Aval[14] and Tham,[18] using the same nozzles, showed that temperature has a second-order effect on spray penetration compared with the effect of gas density. Penetration rate measurements were made by high-speed movie photography and spark photography. The zero time for all penetration measurements is defined as the time at which liquid commences to emerge from the nozzle.

Yule and Aval[19] proposed that cyclic variations in penetration rate measurements are due to a combination of randomness in the atomization process and the irregularity in the spray edge due to turbulence. It is necessary to ensemble-average penetration measurements for a number of pulses, and the experimental data reported here were all obtained from averages of a minimum of 10 spray pulses. It is important to note that scatter is a real effect, due to cyclic variations, with negligible contribution from measurement errors.

The break-up zone structure

Figure 1 represents the hypothesis for the physical structure of the break-up zone, which is based on the information outlined above. The physical structure will be used as the basis for interpreting observations and formulating correlations. The break-up zone is here assumed to be divided into four fairly distinct subzones: From only one to all four of these zones may exist, according to time after commencement of injection. Near the nozzle the *intact column* zone is formed by the column of liquid emerging from the nozzle. This has the basic structure proposed by Castleman, with few, if any, voids within it (apart from possible cavitation bubbles, the existence of which has been proposed by several workers). Aerodynamic forces at its periphery form surface waves that break down via ligaments to form a dense peripheral layer of droplets: This *peripheral atomized zone* obscures photographic investigations of the break-up process. The intact column zone is assumed to stretch to a distance x_{B1}, and beyond this position the column divides (probably chaotically) into ligaments. There is assumed to be a distance, up to $x = x_{B2}$, to the tips of ligaments, which are, at any instant, attached to the liquid column. The value of x_{B2} is, it is proposed, the break-up length that is detected by conductivity probe measurements, such as those described by Arai *et al.*[4] These conductivity investigations define a break-up zone length as the maximum distance from the nozzle over which an electrical current may be passed between the nozzle and a probe or mesh inserted in the spray. In practice there should also be a final part of the break-up zone in which detached ligaments, sheets, and larger droplets continue to subdivide into small droplets. The break-up zone ends at $x = x_B$, where no further subdivision occurs and the fully atomized spray zone commences. It is important to bear in mind that, as shown in Figure 1, well-atomized droplets exist at the periphery of the spray and increasingly toward the center, as the break-up proceeds, i.e., within the break-up length of the spray a significant and increasing proportion of the liquid is in the form of droplets.

Notation

C_1	Empirical constant in penetration rate equation, Equation 1
C_D	Nozzle discharge coefficient, $C_D = U_{inj}(2\Delta P/\rho_L)^{-0.5}$
D_e	Equivalent nozzle diameter, $D_e = D_N(\rho_L/\rho_g)^{0.5}$
D_N	Nozzle orifice diameter
$\dot{m}_g$ and $\dot{m}_L$	Gas and liquid phase mass flow rates through spray cross section
P_g	Gas pressure (absolute)
P_{inj} and $\bar{P}_{inj}$	Injection pressure and mean injection pressure
ΔP	Pressure difference between nozzle inlet and outlet ($\Delta P = P_{inj} - P_g$)
$\underline{\Delta P_0}$ $\overline{\Delta P}$ and $\overline{\Delta P_{0.5}}$	Value at needle valve opening time Average values for whole injection period and first 0.5 ms
Re_B	Reynolds number, $Re_B = U_B D_e/\nu_L$
t	Time after commencement of injection
t_B	Characteristic break-up time
t_I	Initial time, see section on Initial part of break-up zone
U_{inj}	Velocity in nozzle orifice
U_B	Penetration velocity in break-up zone ($\approx x_B/t_B$)
V_F	Volume of fuel injected at time t
V_S	Volume of spray at time t
We_B	Weber number $We_B = \rho_g U_B^2 D_N/\sigma_L$ (also We_J and We_L defined at Equations 7 and 8)
W_g	Gas cross-flow velocity, Figure 1
x_B	Break-up length
x_p	Penetration distance, measured radially from nozzle orifice
Greek symbols	
ρ_g, ρ_L	Densities of gas and liquid fuel, respectively
σ_L	Surface tension of liquid
ν_L	Kinematic viscosity of liquid

Table 1 Principal test conditions

Nozzle diameter D_N (mm)	Length diameter ratio, L/D_N	Needle opening pressure* (bar)	Mean injection pressure* for full opening period (bar)	Mean injection pressure in first 0.5 ms (bar)	Air-equivalent gas pressure†, P_g (bar)	Gas density, ρ_g (kg/m³)	Cross-flow velocity, W_g (m/s)	Vol flow/ pulse (mm³)	Injection duration (ms)
0.265	2	160	210	215	11.8	14.2	13.5	11.4	1.36
					22.2	26.7	0		
					22.2	26.7	8.8		
					22.2	26.7	13.5		
					32.5	39	13.5		
0.213	3.6	220	312	300	5	6	0	10.1	1.5
					25	30	0		
					45	54	0		
0.46	1.65	120	254	245	5	6	0	53.7	1.9
					25	30	0		
					50	60	0		

* Gauge pressures.
† Absolute pressure.

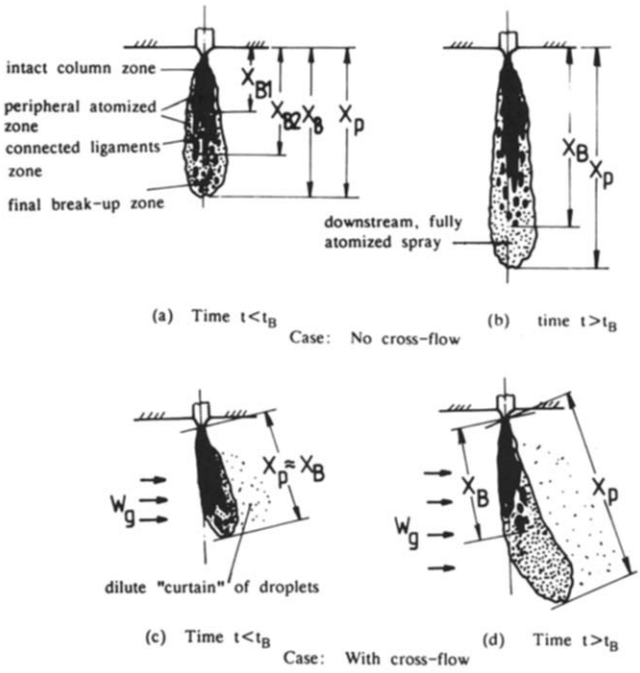

Figure 1 Schematic diagrams showing zones of spray

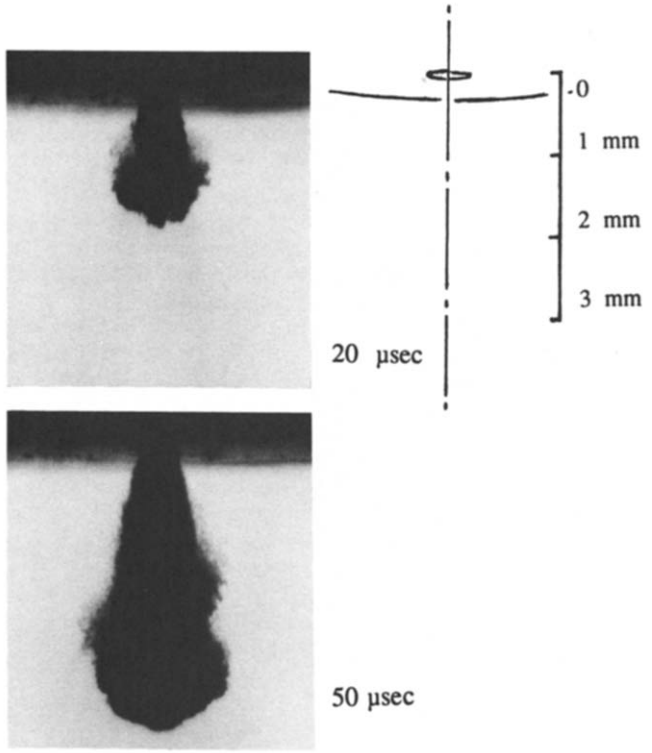

Figure 2 Shadowgraphs showing emergence of spray from 0.46-mm diameter injector orifice, $P_g = 2.2$ MPa and $T_g = 290$ K

During an initial period of penetration, as shown in Figure 1a, the total spray length x_p is essentially equal to the length of the break-up zone at that time, and both parameters, x_B and x_p, are increasing with time. This neglects the thickness of any volume of well-atomized droplets that may precede the break-up zone during this initial period of penetration. At some time $t = t_B$ the break-up zone attains its steady state length, x_B. Although Aval's[14] measurements indicate that this length may change relatively slowly with time, due to variation in nozzle flow rate during the injection period, a constant value x_B is here assumed, in common with the assumption of Arai *et al.*[4] As shown in Figure 1b beyond $t = t_B$ the front edge of the spray is the edge of the fully atomized zone, and the ratio x_p/x_B continues to increase. In agreement with Arai *et al.*[4] one expects that the penetration rate for $t < t_B$ (when the spray consists solely of the break-up zone) should be directly related to the nozzle velocity U_{inj}. However, for $t > t_B$, the fully atomized spray should tend to penetrate according to the proportionality $x_p \propto t^{1/2}$ where the constant of proportionality is related to the spray momentum and gas density. Arai *et al.*[4] have also reported break points in penetration curves, measured using their constant injection pressure apparatus, which they used to measure x_B.

Figure 2 shows high magnification shadowgraphs of the early stages of injection using the 0.46-mm nozzle injecting into gas at 22 bar and 290 K. The gas density under these conditions

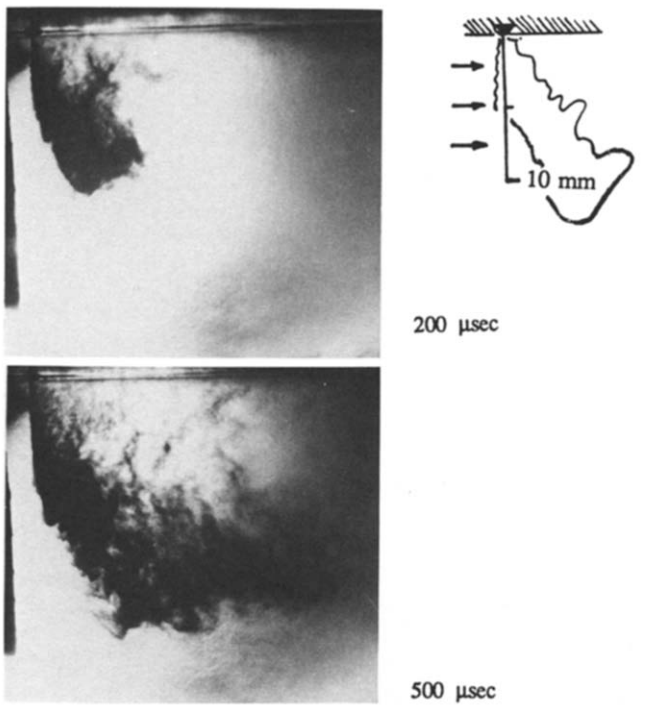

Figure 3 Shadowgraphs of sprays from 0.265-mm injector orifice with 40 m/s cross flow; P_g = 2.5 MPa and T_g = 290 K

is similar to that found in an engine cylinder. Figure 2a, at 20 μs, shows that all of the "spray" consists of an intact liquid column. The aerodynamic forces have distorted the column into an inverted mushroom shape and there is little evidence of droplets. At 50 μs, as shown in Figure 2b, droplets and vapor appear at the periphery of the intact column. At later times this peripheral zone obscures the visibility of the central liquid column and of its breakup.

When there is a cross flow of gas there are distinctive features of sprays that indirectly reveal the presence of the break-up zone. This is particularly so in the case of a strong cross flow, i.e., when cross-flow velocity W_g and local penetration rate dx_p/dt are of the same order of magnitude. Figures 1c and d show diagrammatically the spray structure in the case of a strong cross flow for $t < t_B$ and $t > t_B$, respectively. For $t < t_B$ the upwind side of the spray exhibits little deviation, due to the low drag to inertia ratios of the relatively large liquid masses in the break-up zone. However, deviation of the downwind side is observed, due to the deviation of droplets and the smaller liquid masses. A further distinctive feature, which is often observed photographically is the existence of a dilute curtain of droplets, which moves downwind of the main dense spray zone at a velocity close to that of the cross flow of gas. Presumably droplets in this dilute curtain have become detached from the periphery of the spray as there is no mechanism by which they could be separated from the main central body of the spray by the cross flow.

For $t > t_B$, with cross flow, the deflection of the upwind boundary of the spray is found to increase markedly beyond some downstream position. Figure 3 shows this situation with the spray from the 0.265-mm nozzle injecting into gas at 25 bar with a cross-flow velocity of 40 m/s. Aval[14] has assumed that these upwind boundary break points are related to the length of the break-up zone. The high cross-flow velocities required to make these break points clearly visible appear to affect the atomization process and shorten the length of the break-up zone.

Penetration correlation and break-up time

As described by many authors, the downstream (completely atomized) spray is found to follow a penetration relationship of the form:

$$x_p = C_1\left(\frac{\Delta P}{\rho_g}\right)^{0.25} D_N^{0.5} t^{0.5} \tag{1}$$

This equation is obtained by analogy with an equivalent gas jet, with the same momentum flow rate as that of the liquid flow from the nozzle. However, Arai *et al.*[4] suggested that, in the break-up zone only, an approximately linear relationship between x_p and t should exist. They suggested that the following equation described their break-up zone data, obtained with an impulsively started, constant fuel pressure apparatus:

$$x_p = 0.39(2\Delta P/\rho_L)^{0.5} t \tag{2}$$

Arai *et al.*[4] assumed that the break-up zone ends at the intersection of Equations 1 and 2, which, assuming $C_1 = 3.0$, gave a break-up zone length

$$x_B = 15.8(\rho_L/\rho_g)^{0.5} D_N \tag{3}$$

Assuming the penetration velocity in the break-up zone U_B, given by differentiating Equation 2, and assuming that the break-up time is given by $t_B = x_B/U_B$, Arai *et al.* proposed

$$t_B = 28.65\rho_L D_N/(\rho_g \Delta P)^{0.5} \tag{4}$$

One might expect, intuitively, that $dx_p/dt = U_{inj}$, i.e., that the penetration velocity should equal the liquid exit velocity from the orifice. However, the constant in Equation 2 should then equal C_D, which typically has a value of $0.6 < C_D < 0.7$ rather than 0.39. Arai *et al.* did not discuss this observation, which is considered in more detail later in this paper. Furthermore, their separately presented data on x_B (from penetration rate break points and conductivity probes) were in rather poor agreement with Equation 2. Figure 4 shows typical penetration rate measurements obtained using one of the present injector/pump combinations, and Figure 5 shows the fuel pressure and volume flow rate time histories for this injector. The log/log plot in Figure 4 shows that there is indeed a transition from an approximately $t^{1.0}$ to a $t^{0.5}$ dependency. However, as is generally found with spray penetration data, this is a rather gradual transition, without the clear break point that the two-equation approach of Arai *et al.* implies. Yule *et al.*[20] derived a single equation to match this observed gradual transition from the nozzle to the downstream spray:

$$x_p = C_1(\Delta P/\rho_g)^{0.25} D_N^{0.5} t^{0.5} \tanh[(t/t_B)^{0.6}] \tag{5}$$

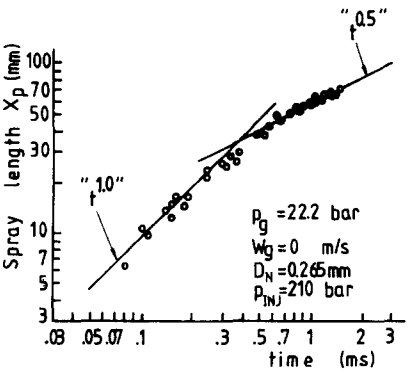

Figure 4 Penetration time history compared with expected proportionalities in the near nozzle and downstream spray zones

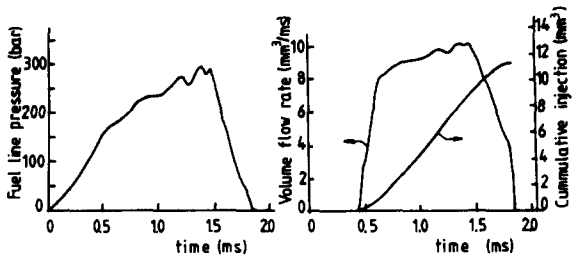

Figure 5 Injection characteristics for injector with 0.265-mm diameter orifice

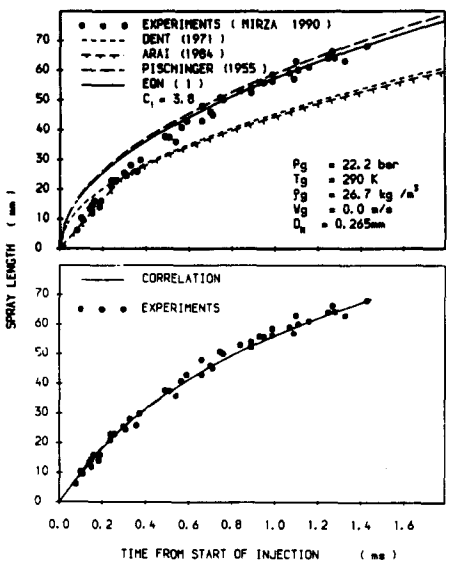

Figure 6 Penetration time history compared with different correlation equations (top) and the new modified correlation of Yule *et al.*[20] (bottom)

where $C_1 = 3.8$ gave best agreement with experimental data. Equation 5 has t_B as an adjustable constant so that, for any given spray, obtaining a best fit between Equation 5 and data provides a value for t_B. One may expect that the value of t_B, found by this technique, should be proportional to, but not necessarily equal to, the time for complete breakup. Figure 6 shows typical penetration data compared with previous penetration curves (upper figure), including those proposed by Pischinger[21] and Dent.[22] Figure 6 also compares the data with the new Equation 5, using the value $t_B = 0.25$ ms for this case. Good agreement is found, and this is the case for all of the penetration data that have been measured.[20] Data for t_B obtained in this way are presented, later in this paper, where they are compared with data obtained by other means. However, attention first is focused on the initial part of the break-up zone, near to the nozzle.

Initial part of break-up zone

It has been described how the penetration velocity U_B during the break-up process is less than the liquid exit velocity U_{inj}. There are two interrelated reasons for this and reference to Figure 2 aids understanding of these reasons. It is seen that, due to aerodynamic drag, the liquid column spreads to form an inverted mushroom shape immediately after leaving the nozzle. This itself must result in a deceleration from the initial liquid velocity U_{inj}. Furthermore, an impulsively started gas jet forms a starting vortex, and it is likely that a similar recirculating zone exists within the front region of the liquid column. A gas jet starting vortex moves at approximately half the jet exit velocity. One would expect the velocity U_B to be intermediate in value between $U_{inj}/2$ and U_{inj} for the case of the liquid column. In addition one would expect U_B to be dependent on the gas density that affects the drag on the column and thus its shape in the initial part of the penetration history: At low gas density one would expect $U_B \simeq U_{inj}$.

This has been investigated by examining the present data, in the near nozzle region, by using a relationship similar to Arai's Equation 2:

$$x_p = K(2(P_{inj} - P_g)/\rho_L)^{0.5}t \qquad (6)$$

The constant K, in Equation 6, is equal to 0.39 according to Arai *et al.* During the initial period of injection P_{inj} is increasing. If there is a continuous liquid column one would expect some effect on the penetration rate due to this. Furthermore, as the needle valve opens C_D increases from zero to its fully open value; however, this increase occurs over a period less than 0.1 ms. As a first approximation Equation 6 has been applied to the data and P_{inj} has been allowed to vary according to the measured fuel pressure signals. Figure 7a shows, for the case of the 0.265-mm orifice diameter injector, comparisons between

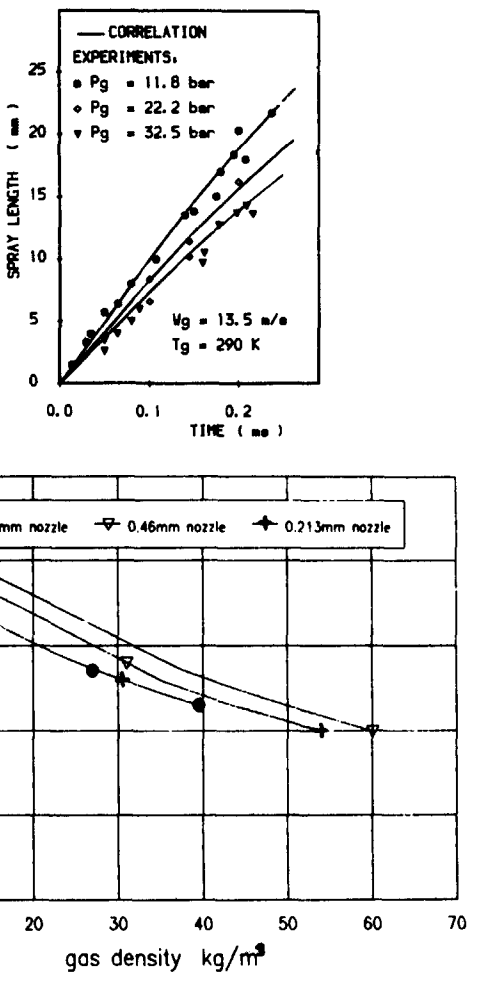

Figure 7 (a) Penetration measurements for 0.265-mm nozzle compared with near nozzle penetration equation, Equation 6; and (b) measured values of K, from Equation 6, as a function of gas density

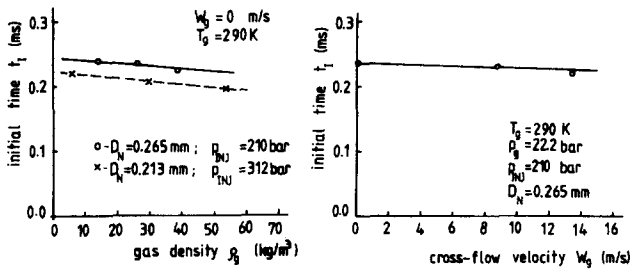

Figure 8 Initial time for which Equation 6 agrees with measured penetration as function of gas density (left) and cross-flow velocity (right)

Equation 6 and data for variation in the gas pressure. For each condition, in Figure 7, the value of K is constant (i.e., independent of time); however, the value of K is chosen to give best fit with the data. Figure 7b shows values of K, obtained in this way, plotted against gas density. It is seen that K decreases from a value very close to 0.65 (which is the value of C_D for the nozzle) to values similar to the value 0.39 quoted by Arai. It is thus clear that the earlier arguments regarding the initial penetration of the liquid column are correct. The dependency of U_B/U_{inj} on the liquid and gas conditions is addressed again later in the paper. Increasing the cross-flow velocity also tends to decrease K, and thus penetration rate, in a similar way to the decreased penetration rate in the downstream spray zone, as described by Yule *et al.*[20] The effect is relatively small, at least for cross-flow velocities less than 20 m/s.

One might expect that the agreement of Equation 6 with data should be best in the intact column zone of the break-up region, i.e., $0 \leqslant x \leqslant x_{B1}$ approximately. Curve fits of the penetration data have been compared with Equation 6 and the times at which the disagreement becomes greater than or less than 5 percent have been derived. These will be referred to as the *initial times* t_I and Figure 8 plots these data as a function of gas density and cross-flow velocity for the three different nozzle-pump combinations (see Table 1). It is seen that there is a relatively small trend for t_I to decrease with both increasing gas density and increasing cross-flow velocity. It is remarkable that all measurements of t_I lie in the narrow range $0.2 \text{ ms} < t_I < 0.25 \text{ ms}$; however, it should be noted that the distances downstream, corresponding to these times, have very much more variation. Further discussion of this observation is made after presentation of the break-up times and lengths derived using other techniques.

Break-up parameters derived from overall void fraction of spray

As a spray pulse penetrates downstream, without a gas cross flow, it exhibits a sharp boundary in photographs, within which is all of the injected fuel. The spray volume within this boundary, V_S, may be measured as a function of time from photographs and by assuming axisymmetry. The volume of fuel V_F, injected into the spray, is also known as a function of time. If, for injection into cold gas, one neglects the mass fraction of vaporized fuel one may compute the overall void fraction, which is, as a percentage, $100(1 - V_F/V_S)$ or the liquid fraction (nonvoid fraction) which is $100V_F/V_S$. This latter quantity is found to be more convenient when presenting data, and $100V_F/V_S$ should clearly start with a value 100 percent near the orifice (ignoring any cavitation). For the intact column zone (see Figure 1), i.e., penetration up to $x_p = x_{B1}$, one expects a relatively slow reduction in $100V_F/V_S$. There should then be a more rapid reduction up to the end of the break-up zone, at $x_p = x_B$, and thereafter, ideally, the void fraction should decrease in a similar fashion to that for a turbulent gas jet containing a suspension of particles. Now such a gas jet penetrates as $x_p \propto t^{0.5}$ so that the volume in the jet (and thus in the downstream spray) should follow the proportionality $V_S \propto x_p^3$ so that $V_S \propto t^{1.5}$. For a constant injection rate of particles one has $V_F \propto t$ so that in the downstream spray one expects, approximately, the proportionality $100V_F/V_S \propto t^{-0.5}$. Alternatively, in terms of the penetration distance, one expects $100V_F/V_S \propto x_p^{-1.0}$.

Tham[18] has processed photographic penetration data in this way and, as an example, Figure 9 shows log/log plots of the overall nonvoid fraction, as a function of penetration distance, for the nozzle with $D_N = 0.213$ mm, and for variation of the density of gas into which the sprays are injected. It is seen that there is indeed a tendency toward the proportionality $100V_F/V_S \propto x_p^{-1.0}$ beyond a break-point position, which moves nearer to the nozzle as the gas density is increased. The break points corresponding to these positions are more clearly defined than those in penetration rate curves (compare with Figure 4 for example). By deriving the nonvoid fraction, which is a dimensionless parameter, it is likely that the "smearing" effect, which the time varying nozzle flow rate has on the penetration rate break point, is being partially removed. Each data set, in Figure 9, has been fitted by three straight lines. Apart from the downstream spray zone, this is rather arbitrary. However, these lines are seen to give excellent fits to the data and they do reveal another break point closer to the nozzle. This break point should, it is proposed, indicate the end of the intact column part of the break-up zone and, as expected, its position moves closer to the nozzle as the gas density is increased. The nonvoid fraction appears to follow, quite closely, the proportionality $100V_F/V_S \propto x_p^{-2.0}$ between the two break points; however, there is no a priori justification of this proportionality. As should be the case, there is a strong tendency for the measurements for all sprays to collapse on each other beyond the second break point. This shows that the downstream sprays essentially "forget" the break up process, although the small deviation, from the rest of the data, found for the lowest gas pressure is probably indicative of large droplets for this case that do not follow the turbulent gas flow. Assuming that the second break point is a measure of the total length of the break-up zone, Figure 10 shows values of x_B and t_B obtained from void-fraction data for two injectors. It can be seen that as for the t_I data in Figure 8, t_B appears to be

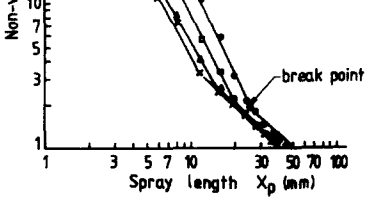

Figure 9 Overall nonvoid fraction for sprays as function of penetration distance using 0.213-mm diameter nozzle (from Tham[18])

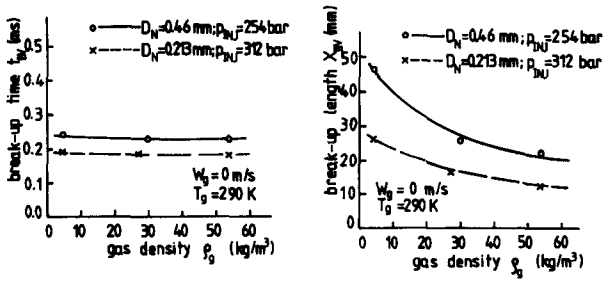

Figure 10 Break-up times (left) and lengths (right) measured from break points in overall void fraction measurements

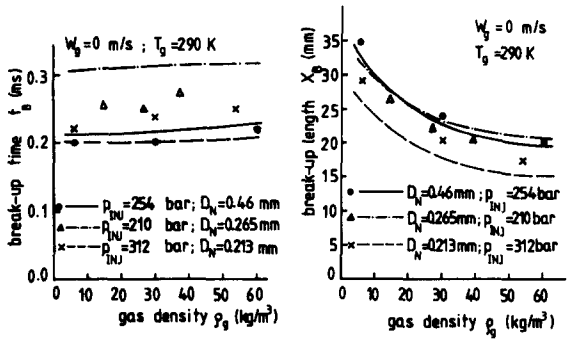

Figure 11 Break-up times (left) and lengths (right) derived by curve fits to penetration correlation Equation 5 of Yule *et al.*[20] Lines represent Equations 12, for t_B, and 8, for x_B

insensitive to ρ_g and differs little for the two nozzle diameters, $D_N = 0.213$ mm and $D_N = 0.46$ mm. There is a clear reduction of x_B with increasing gas density, which, at first sight, appears to follow an approximately $x_B \propto \rho_g^{-0.5}$ trend proposed by Arai *et al.*[4] (Equation 3). It should be noted that Arai's proposed proportionality $t_B \propto \rho_g^{-0.5}$ (Equation 4) is not supported by the present data. Thus, the data show that although, for a given nozzle, the break-up time varies little with gas density, the break-up length decreases with increasing gas density. This is primarily due to the reduction of the intact column zone velocity U_B, with increasing gas density, which has been discussed in the previous section on Penetration correlation and break-up time. Referring back to Figure 9 the intact column length x_{B1} appears to be 20($\pm$5) percent of the total break-up length x_B for the present injectors. The values of t_I and t_B obtained by using two different techniques (Figures 8 and 10) appear to agree remarkably well, and this leads to the conclusion that the initial zone penetration equation, Equation 6, is applicable further downstream than the end of the intact column length.

Break-up parameters derived from penetration correlation for full spray

As described previously, curve fitting Equation 5 to penetration data provides a value for t_B. Figure 11 shows values of both t_B and x_B derived by this procedure for the three different nozzle-pump combinations and for variation in gas density. There is good general agreement between t_B values derived by this procedure and those derived from the void-fraction measurements. Although a constant factor of proportionality between t_B (or x_B) derived by the two techniques should be expected, the observation that this factor appears to be near unity is, to some extent, due to a providential choice of the $\tanh[(t/t_B)^{0.6}]$ term in Equation 5. The lines in Figure 11 are correlation equations, described in the next section. Figure 12 shows the break-up length, at one gas pressure, for the three different nozzle diameters, showing a gradual increase with nozzle diameter. However, the data are derived for the three different mean fuel injection pressures, corresponding to the normal operating conditions of each injector-pump combination, and the differing effects of injection pressure and nozzle diameter must also be considered. This is done below. Measurements of t_B and x_B with variation of cross-flow velocity, in the range $0 \leqslant Wg \leqslant 14$ m/s, show little variation.

Correlation equations for break-up zone parameters and discussion

Figure 13 shows the variation of x_B and t_B as functions of ρ_g given by Equations 3 and 4, which are the correlations proposed by Arai *et al.*[4] These are evaluated for both 0.213- and 0.460-mm diameter nozzles at their respective operating conditions. As both Equations 3 and 4 have a dependency on D_N, to the power 1.0, and a dependency on ρ_g, to the power -0.5, only one curve needs to be shown for each case. Comparison with both the void-fraction measurements, in Figure 10, and the penetration curve-fit measurements, Figure 11, reveals

(1) an approximately $\rho_g^{-0.5}$ dependency for x_B appears to be justified;
(2) Equations 3 and 4 appear to overestimate the dependency on D_N of x_B and t_B;
(3) Equation 4 does not reflect the observed insensitivity of t_B to the gas density.

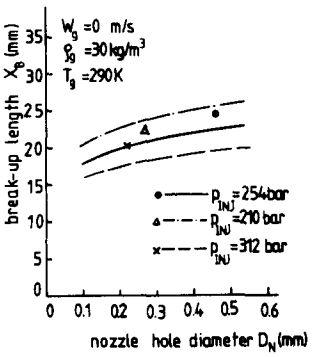

Figure 12 Break-up lengths, at one gas density, as a function of nozzle diameter. Lines represent Equation 8 at the relevant mean injection pressures

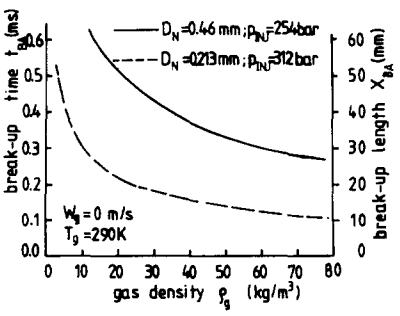

Figure 13 Break-up times and lengths, evaluated for the present operating conditions, using Equations 3 and 4 of Arai *et al.*[4]

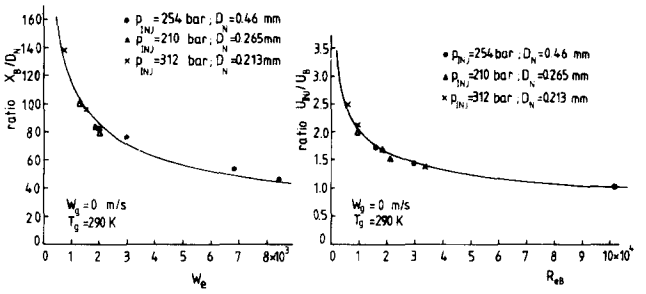

Figure 14 Break-up length (left) and characteristic break-up zone velocity (right) *versus* break-up zone Weber number and Reynolds number, respectively. Lines represent Equations 8 and 10

Arai *et al.*[4] themselves indicated that their equations, although convenient in form, do not truly reflect all of their data. In particular the overestimate of the dependency on D_N can also be observed in their comparisons with their penetration break-point measurements of x_B.

There has been little attempt, apart from the work of Arai *et al.*, to derive relationships for the break-up length in the "atomization" regime found for practical injection conditions. However, there are empirical and also theoretical relationships for the other regimes of liquid column breakup, which occur at lower values of U_{inj}. Zanelli[16] has reviewed these relationships and he has also introduced new information on the possible role of cavitation in the break-up process. His results indicate that Haenlein's[2] "second wind (SW) regime" occurs for a value of nozzle Reynolds number, $\mathrm{Re}_L = U_{inj}D_N/\nu_L$, less than approximately 2,000 at engine conditions. This situation is unlikely to occur in practice, where generally $\mathrm{Re}_L \gg 2{,}000$; however, the relative orderly break-down process in the SW regime led to a proposal:

$$x_L/D_N = (\mathrm{A}/\mathrm{We}_J)(\rho_L/\rho_g)^{0.5}(1/g) \tag{7}$$

where x_L is the length of the undisturbed liquid column, which is clearly visible in the SW regime, A is a constant, We_J is the Weber number $\rho_g U_{inj}^2 D_N/\sigma_L$, and g is "a function of $\mathrm{We}_L/\mathrm{Re}_L$" where We_L is the Weber number $\rho_L U_{inj}^2 D_N/\sigma_L$. In the atomization regime, at higher Re_L, one might expect any direct dependency of breakup on liquid viscosity to be small, i.e., that g is probably fairly constant. Fitting the present break-up length data by, primarily, a negative power of the Weber number was thus explored. It was found that a Weber number We_B based on the penetration velocity U_B in the initial break-up zone, gave an excellent correlation with the present data so that

$$x_B/D_N = 2.8 \times 10^4 \mathrm{We}_B^{-0.46} \tag{8}$$

where $\mathrm{We}_B = \rho_g U_B^2 D_N/\sigma_L$.

The method of deriving U_B from the near-nozzle zone penetration measurements has been described in the section on the Initial part of break-up zone. It is clear that for Equation 8 to be useful one requires a further correlation for U_B and this also is presented. Figure 14 compares the present measurements of x_B/D_N as a function of We_B, derived by curve fitting Equation 5, and Equation 8. There is seen to be good agreement for all of the nozzles and operating conditions. It has been described how the value of U_B is approximately equal to the nozzle exit velocity U_{inj}, at low gas density, but that it decreases in value so that at high gas density one has a value similar to, or lower than, the value that one may infer from Arai's Equation 2, i.e.,

$$U_B/U_{inj} \simeq (0.39/C_D) \simeq 0.6 \tag{9}$$

for a typical value of $C_D = 0.7$.

It was found that the optimal correlation is based on a Reynolds number Re_B, which is based on the velocity U_B and the equivalent nozzle diameter $D_e = D_N(\rho_L/\rho_g)^{0.5}$ so that

$$U_{inj}/U_B = 31.7\mathrm{Re}_B^{-0.3} \tag{10}$$

where $\mathrm{Re}_B = U_B D_e/\nu_L$.

This equation is compared with the present measurements for three nozzles in Figure 14 and, once again, there is good agreement. As with all empirically derived correlations care must be taken applying Equation 10 outside the range covered by the present experiments. In particular, Equation 10 should only be applied up to $\mathrm{Re}_B = 10^5$, where $U_{inj}/U_B = 1.0$, as one cannot have values of U_B greater than U_{inj}.

The break-up time t_B is needed, for example, when using the general penetration equation, Equation 5, and this may be derived with sufficient accuracy by assuming

$$t_B = x_B/U_B \tag{11}$$

and Equations 8 and 10 thus give

$$t_B = 8.9 \times 10^5 \mathrm{We}_B^{-0.46}\mathrm{Re}_B^{-0.3} D_N/U_{inj} \tag{12}$$

Although Equations 8 and 10 appear straightforward this is to some case misleading as, for example, U_B occurs both on the left-hand side of Equation 10 and also, via Re_B, on the right-hand side. One might consider that a process of iteration would thus be required to derive a value for U_B for particular operating conditions. However, it is probably more useful to rewrite Equations 8, 10, and 12 in explicit forms for x_B, U_B, and t_B and substituting for the typical properties of diesel fuel: $\nu_L = 10^{-5}\ \mathrm{m^2\ s^{-1}}$, $\sigma_L = 0.03\ \mathrm{Nm^{-1}}$ and $\rho_L = 861\ \mathrm{kg^{-3}}$. This gives

$$U_B = 0.034 D_N^{0.43} \rho_g^{-0.21} \Delta P^{0.71} \tag{13}$$

$$x_B = 1.26 \times 10^4 D_N^{0.15} \rho_g^{-0.26} \Delta P^{-0.66} \tag{14}$$

and

$$t_B = 3.75 \times 10^5 D_N^{-0.28} \rho_g^{-0.05} \Delta P^{-1.37} \tag{15}$$

Equations 13–15 must be used with consistent SI units; however, they are obtained from dimensionally correct correlations. These equations display certain interesting features. For example Equation 15 shows a very weak dependency of break-up time on the gas density, which is a feature of all the measurements that have been described. There is a stronger inverse dependency of break-up length x_B on gas density although the power (-0.26) is less than the power in Arai's Equation 3. The dependency of both x_B and t_B on the orifice size D_N is substantially less than the linear dependency proposed by Arai and this is in agreement with both the present measurements and those of Arai. The relatively strong dependency of both x_B and t_B on the pressure differential ΔP is also of interest. As can be seen in Equations 3 and 4, Arai's equations provide a dependency of t_B and $\Delta P^{-0.5}$ but no dependency of x_B on ΔP. Equation 14 indicates that increasing ΔP should be the most successful method of reducing x_B. However, this is not quite so straightforward because, for example, increasing ΔP requires a reduction in D_N to maintain the same nozzle flow rate. However, the relatively low power of D_N, in Equation 14, does result in a net reduction in x_B. It is worthwhile at this point stating that maintaining a relatively high value of x_B could well be a primary design requirement, as this ensures rapid initial penetration, which is important for smaller engines.

Figure 15 shows how the new correlations predict the break-up time and break-up length as a function of injection pressure for the three nozzles and for injection into air at 25 bar and 290 K. There is reasonable agreement for the relatively narrow range of injection pressures that has been used; however, care must be taken extrapolating the injection

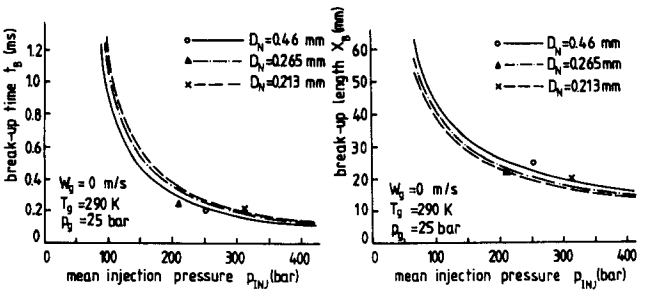

Figure 15 Break-up time (left) and length (right) as functions of injection pressure for the three nozzles. Lines represent Equations 12 and 8, respectively

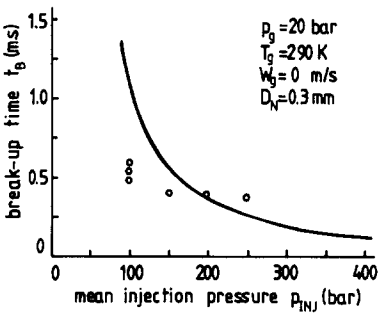

Figure 16 Break-up time measured from the penetration curve break points of Arai *et al.*[4] compared with Equation 12

pressure below approximately 150 bar, where break up is undoubtedly tending to be via the SW mechanism rather than the atomization mechanism, which is the normal regime for practical diesel injection systems. The break-point measurements of Arai *et al.*[4] of x_B and t_B were extended down to an injection pressure of 100 bar and t_B values, from their penetration curves, and are compared with Equation 12 in Figure 16. There is satisfactory agreement at the higher injection pressures, but the correlation appears to overestimate the break-up time at lower injection pressures, for the reasons that have been described.

Referring back to Figure 11 the correlations are included in these figures for x_B and t_B. In general the agreement is better for x_B than for t_B. This is likely to be due partly to the simplified relationship for t_B, i.e., Equation 12. The relationships between x_B and D_N, for the different injection pressures, are included in Figure 12. It is seen that the data for the three operating conditions lie reasonably close to their respective curves, although clearly a wider range of data is desirable.

It is interesting to compare the break-up length data of Arai *et al.*,[4] measured using pulsed water sprays and a conductivity probe, with the new correlations. Figure 17a compares Equation 8 with Arai's measurements of break-up length for two injection pressures and for various nozzle diameters in the range $0.1 \leqslant D_N \leqslant 0.4$ mm. All measurements were made with injection into air at a pressure of 30 bar and temperature 290 K. Although the equations greatly overestimate the conductivity probe measurements of break-up length, the general shapes of the curves, and the increase with increasing injection pressure, seem to correctly reflect the measurement trends. To check this Figure 17b compares Arai's measurements (vertical axis) and the relevant values from Equation 8 (horizontal axis). It can be seen that there is a clear correlation between the measurements and Equation 8 and, on average, Arai's measurements are 35 percent of the values obtained from

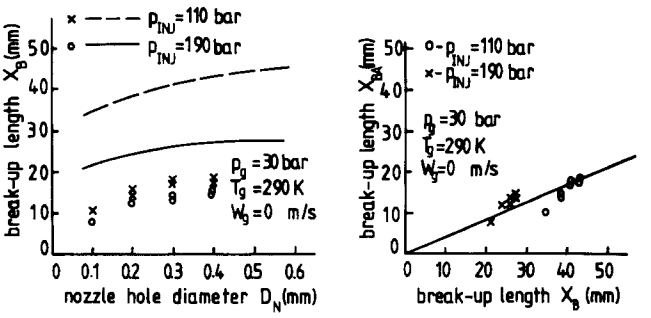

Figure 17 (a) Measurements of break-up length by Arai *et al.*[4] using a conductivity probe; lines represent Equation 8. (b) Comparison of Arai's measurements (ordinate) and prediction of Equation 8 (abscissa)

Equation 8. If, as described in the section on the break-up zone structure, Arai's conductivity probe measurements are representative of the length x_{B2} this implies that $x_{B2} \simeq 0.35x_B$. It is recalled that the void fraction data were used to deduce that the intact column length is given by $x_{B1} \simeq 0.2x_B$.

The forms of the correlations, for x_B, U_B, and t_B, imply that aerodynamic forces, via a Weber number, are principally responsible for the break-up process, and other factors, such as fluid viscosity, have indirect effects in that they affect the shape and deceleration of the initial liquid column, and thus the value of U_B. No attempt has been made here to measure or analyze the effects of initial turbulence or cavitation within the nozzle on the break-up process. Zanelli[16] has reviewed the relatively scarce experimental and theoretical information on these effects. According to his summary graphs one would expect that cavitation might occur, only for the lower gas densities for the present tests, i.e., for approximately $\rho_g < 15$ kg/m^3. These are clearly not typical engine conditions. As has been described by Yule and Aval,[19] the liquid flow leaving the orifice should be similar to that of a fully turbulent pipe flow, bearing in mind the high Reynolds number and rather convoluted liquid path through the nozzle. If a nozzle design is such that a laminar flow is possible then clearly the present break-up correlation equations should be used with caution, and they are likely to underestimate the break-up lengths and times. There seems to be some ambiguity on the role of the length of the exit orifice on the break-up process, i.e., the effect of L/D_N. The measurements of Arai *et al.*[4] indicate that L/D_N can have quite a strong effect on the initial spray angle, depending on the nozzle design and value of U_{inj}, with a maximum tending to occur in the range $3 \leqslant L/D_N \leqslant 5$. Their results indicate relatively little effect of L/D_N on the break-up length or on the droplet sizes. It thus seems likely that L/D_N affects the initial ranges of angle of droplet trajectories at the periphery of the flow (outside the initial liquid column) without having a major effect on the main break-up process.

Conclusions

Data derived from three injector-pump combinations have been processed in several ways to derive information on spray break up. The data show that the relative lengths of the intact column and continuous liquid path zones are, respectively, approximately 20 and 35 percent of the full break-up length.

Correlation equations, based on suitable Weber and Reynolds numbers, give good general agreement with the measurements of break-up length, break-up time, and initial penetration velocity. The equations are consistent with the

relatively scarce published measurements in this field and they provide a sound basis for the validation of CFD submodels of the break-up zone.

References

1 Castleman, R. A. Mechanism of atomization accompanying solid injection. N.A.C.A. Report no. 40, 1932

2 Haenlein, A. On the disruption of a liquid jet. N.A.C.A. T.M., 659, 1932

3 Hiroyasu, H., Shimizu, M. and Arai, M. The break-up of high speed jet in a high pressure gaseous atmosphere. *Proc. 2nd Int. Conf. on Liquid Atomization and Spray Systems*, 1982, 69–74

4 Arai, M., Tabata, M., Hiroyasu, H. and Shimizu, M. Disintegrating process and spray characterization of fuel jet injected by a diesel nozzle. SAE Tech. Paper 840275, 1984

5 Yule, A. J. Diesel spray atomisation and vaporisation. *Report to Joint Research Committee of European Automobile Manufacturers*, UMIST, 1984

6 Yule, A. J., Aval, S. M., Tham, S. Y. and Mo, S.-L. Diesel spray structure. *Proc. ICLASS-85*, Inst. Energy, London, UK, 1985

7 Ishikawa, M. and Murakami, T. *Proc. ICLASS-82*, 75-81, University of Wisconsin, Madison, WI, USA, June 1982

8 O'Rourke, P. J. and Bracco, F. V. Modelling of drop interactions in thick sprays and a comparison with experiments. *Inst. Mech. Engineers*, Publication 1980-9, 101–116, 1980

9 Watkins, A. P. Three-dimensional modelling of gas flow and sprays in diesel engines. *Computer Simulation for Fluid-Flow, Heat and Mass Transfer and Combustion in Reciprocating Engines* (N. C. Markatos, Ed.), Hemisphere, Washington, DC, 1989

10 Yule, A. J. and Watkins, A. P. Measurement and modelling of diesel sprays. *Atomization and Sprays*, 1991, **1**, 445–469

11 Reitz, R. D. Modelling atomization processes in high pressure vaporizing sprays. *Atomisation and Spray Tech.*, 1988, **3**, 309–337

12 Yule, A. J. and Aval, S. M. A technique for velocity measurement in diesel sprays. *Combustion and Flame*, 1989, **77**, 385–394

13 Pitcher, G. and Wigley, G. Velocity and dropsize measurements in fuel sprays in a direct injection diesel engine. *Proc. Int. Conf. Mechanics of Two-Phase Flows*, National Taiwan University, Taipei, Taiwan, June 1989

14 Aval, S. M. A study of pulsed sprays in a high pressure and temperature gas cross-flow. Ph.D. thesis, University of Manchester (UMIST), UK, 1990

15 Ragucci, R., Cardamone, P., Cavaliere, A. and Noviello, C. Investigation on evaporating diesel sprays. *Proc. 6th Ann. Conf. ILASS-Europe*, University of Pisa, Italy, July 1990

16 Zanelli, S. Behaviour of a liquid jet near the nozzle. *Proc. ICLASS-88*, Fuel Soc. of Japan, Sendai, August 1988

17 Xu, M. and Hiroyasu, H. Development of a new optical technique for measuring diesel spray penetration. SAE Tech. Paper 902077, October 1990

18 Tham, S. Y. The study of diesel spray structure and penetration in high pressure and temperature quiescent gas. Ph.D. thesis, University of Manchester (UMIST), UK, 1986

19 Yule, A. J. and Aval, S. M. Cyclic variations in diesel sprays. *FUEL*, 1989, **58**, 1558–1564

20 Yule, A. J., Mirza, M. R. and Filipovic, I. Correlations for diesel spray penetration including the effects of the break-up zone. *Proc. ICLASS-91*, Nat. Inst. Standards and Technology, Gaithersberg, MD, USA, July 1991

21 Pischinger, F. Verfahren zur untersuchung von diesel-einspritzstrahlen. aschBau Warmew, 1955, 10

22 Dent, J. C. A basis for the comparison of various experimental methods for studying penetration. *SAE Trans.*, 80, Paper No. 710571, 1971